Journal of Solid Mechanics Vol. 4, No. 3 (2012) pp. 267-276

Nonlinear Vibration and Instability Analysis of a PVDF Cylindrical Shell Reinforced with BNNTs Conveying Viscose Fluid Using HDQ Method

R. Kolahchi[1], A. Ghorbanpour Arani[1,2*]

[1]*Faculty of Mechanical Engineering, University of Kashan, Kashan, Islamic Republic of Iran*
[2]*Institute of Nanoscience & Nanotechnology, University of Kashan, Kashan, Islamic Republic of Iran*

Received 9 July 2012; accepted 14 September 2012

ABSTRACT

Using harmonic differential quadrature (HDQ) method, nonlinear vibrations and instability of a smart composite cylindrical shell made from piezoelectric polymer of polyvinylidene fluoride (PVDF) reinforced with boron nitride nanotubes (BNNTs) are investigated while clamped at both ends and subjected to combined electro-thermo-mechanical loads and conveying a viscous-fluid. The mathematical modeling of the cylindrical shell and the resulting nonlinear coupling governing equations between mechanical and electrical fields are derived using Hamilton's principle based on the first-order shear deformation theory (FSDT) in conjunction with the Donnell's non-linear shallow shell theory. The governing equations are discretized via HDQ method, and solved to obtain the resonant frequencies and critical flow velocities associated with divergence and flutter instabilities as well as re-stabilization of the system. Results indicate that the internal moving fluid plays an important role in the instability of the cylindrical shell. Application of a smart material such as PVDF improves significantly the stability and vibration of the system.

© 2012 IAU, Arak Branch. All rights reserved.

Keywords: Nonlinear vibration; Instability; Electro-thermo-mechanical loadings; Viscous-fluid-conveying; HDQM

1 INTRODUCTION

CIRCULAR cylindrical shells are used in a great variety of engineering applications in mechanical, and process industries, ranging from storage and transport of high-pressure gases and liquids, to much smaller nano-scale applications in smart structures such as sensors and actuators. Hence, cylindrical shells are required to be modeled mathematically. A good understanding of their mechanical behavior, including vibration, bending and wave propagation response, is therefore required for successful design practices. Improving mechanical behaviors (e.g. increasing stability and reduction of weight) of such structures in composite applications have also received considerable attention amongst researchers in the last two decades. Most studies to-date are limited to linear vibration, despite the fact that deformations of cylindrical shell are nonlinear in nature. Having considered the geometrical nonlinearities, more precise dynamic properties of cylindrical shell could be obtained to extend the engineering applications, especially in nano-composites.

Effects of internal flow on the vibration of a cylindrical shell were investigated by many authors [1-3]. None of these studies considered smart structures such as PVDF, a new polymeric piezoelectric material offering advantages including flexibility in thermoplastic conversion techniques, excellent dimensional stability, abrasion and corrosion

* Corresponding author. Tel.: +98 9131626594; Fax: +98 36155912424.
E-mail address: aghorban@kashanu.ac.ir (A.Ghorbanpour Arani).

© 2012 IAU, Arak Branch. All rights reserved.

Archive of SID
www.SID.ir

resistance, high strength, ability to maintain the superior mechanical properties at elevated temperature [4-6]. In previous works , Ghorbanpour Arani et al. [7, 8] carried out a stress analysis in cylinder and spheres made from piezoelectric materials using analytical method and ANSYS software. In another study, the embedding of piezoelectric materials in the form of fibers into a polymer matrix was implemented by Bent et al. [9]. Free vibration of composite plates and cylindrical shell panels were studied by Matsuna [10] using a higher-order theory. Free vibration and buckling analysis of composite cylindrical shells conveying hot fluid was proposed by Kadoli and Ganesan [11]. Vibration and buckling of cross-ply laminated composite circular cylindrical shells were studied by Messina and Soldatos [12] based on a global higher-order theory. Lately, the authors extended the work of Mosallaie Barzoki [13] to include electro-thermo-mechanical buckling analysis of a smart composite cylindrical shell made by PVDF reinforced with BNNTs equipped with an elastic core. When nonlinearities are taken into account, no analytical solution could be employed to obtain the vibration frequency. Hence, a numerical solution should be tried, and DQM introduced by Belman et al. [14, 15] is one such method with the advantage of offering good accuracy with limited number of grid points. Successful DQM applications in engineering problems such as vibration analysis and buckling have been developed and verified by several authors [16-18]. HDQM was later developed by Sterize et al. [19] and Liew et al. [20], presenting even more improved accuracy with respect to DQM, less computation time and consequently less memory space from the computer [21].

A number of studies have used HDQM for linear and nonlinear vibration of one dimensional beam and two dimensional plates. In this article, HDQM is used for the first time in the nonlinear vibration of two dimensional cylindrical shells, with a view to apply this to a smart composite structure, such as PVDF as the matrix and BNNT as the reinforce, conveying a viscous fluid. Due to the specific application in mind as sensor or actuator, both in nanoscale and even larger gas and oil transmission pipes, the influences of fluid velocity, the shell geometrical characteristics and material of construction are investigated here.

2 THEORETICAL BASES

A schematic diagram, of a piezoelectric polymeric cylindrical shell with two fixed ends for conveying viscous fluid with density ρ_f and dynamic viscosity μ is shown in Fig. 1 in which geometrical parameters of length, L, radius, R, thickness h and density ρ are also indicated. Using FSDT in conjunction with the Donnell's non-linear shallow shell theory [22], the constitutive equation may be arbitrarily combined as follows [7, 8]

$$\begin{Bmatrix}\sigma_{xx}\\ \sigma_{\theta\theta}\\ \sigma_{x\theta}\\ D_{xx}\end{Bmatrix}=\begin{bmatrix}C_{11} & C_{12} & 0 & e_{11}\\ C_{12} & C_{22} & 0 & e_{12}\\ 0 & 0 & C_{66} & 0\\ e_{11} & e_{12} & 0 & -\in_{11}\end{bmatrix}\left[\begin{matrix}\begin{Bmatrix}\dfrac{\partial u}{\partial x}+\dfrac{1}{2}\left(\dfrac{\partial w}{\partial x}\right)^2\\ \dfrac{\partial v}{R\,\partial\theta}+\dfrac{w}{R}+\dfrac{1}{2}\left(\dfrac{\partial w}{R\,\partial\theta}\right)^2\\ \dfrac{\partial u}{R\,\partial\theta}+\dfrac{\partial v}{\partial x}+\dfrac{\partial w}{\partial x}\dfrac{\partial w}{R\,\partial\theta}\end{Bmatrix}-z\begin{Bmatrix}\dfrac{\partial^2 w}{\partial x^2}\\ \dfrac{\partial^2 w}{R^2\partial\theta^2}\\ 2\dfrac{\partial^2 w}{R\partial x\partial\theta}\end{Bmatrix}-\begin{Bmatrix}\alpha_{xx}\\ \alpha_{\theta\theta}\\ 0\end{Bmatrix}\Delta T\\ \dfrac{\partial\varphi}{\partial x}\end{matrix}\right], \quad (1)$$

where $\sigma_{ij}\ (i,j=x,\theta)$ and D_{xx} are stresses and axial electric displacement (axially polarized) as well as u,v,w are the displacements of a arbitrary point of the shell in the axial, circumferential and radial directions, respectively. Also, C_{ij}, e_{ij}, $\in_{ii}$ $(i,j=1,...6)$, correspond respectively to composite equivalent elastic constants, piezoelectric constants, and dielectric (determined using the micromechanical model [13], and $\alpha_{ii}\,(i=x,\theta)$, ΔT and ϕ are thermal expansion coefficient, temperature difference and electric potential, respectively.

© 2012 IAU, Arak Branch

www.SID.ir

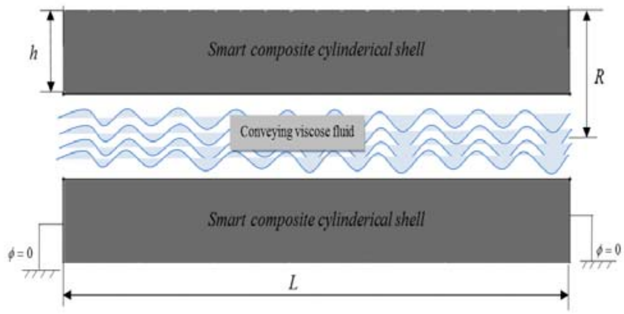

Fig. 1
Hollow smart composite circular cylindrical shell conveying fluid.

2.1 Energy method

The total potential energy of the PVDF pipe is the sum of strain energy, kinetic energy and work down by flowing fluid is expressed below where the strain energy is [13, 22]

$$U=\int_{-\frac{h}{2}}^{\frac{h}{2}}\int_A\left(\sigma_{xx}\left(\frac{\partial u}{\partial x}+\frac{1}{2}\left(\frac{\partial w}{\partial x}\right)^2-z\frac{\partial^2 w}{\partial x^2}\right)+\sigma_{\theta\theta}\left(\frac{\partial v}{R\partial\theta}+\frac{w}{R}+\frac{1}{2}\left(\frac{\partial w}{R\partial\theta}\right)^2-z\frac{\partial^2 w}{R^2\,\partial\theta^2}\right)\right.$$
$$\left.+\sigma_{x\theta}\left(\frac{\partial u}{R\partial\theta}+\frac{\partial v}{\partial x}+\frac{\partial w}{R\partial\theta}\frac{\partial w}{\partial x}-2z\frac{\partial^2 w}{R\partial\theta\,\partial x}\right)+D_x\frac{\partial\varphi}{\partial x}\right)dz\,dA, \qquad (2)$$

and the kinetic energy is [22]

$$K=\frac{\rho}{2}\int_v\left((\frac{\partial u}{\partial t})^2+(\frac{\partial v}{\partial t})^2+(\frac{\partial w}{\partial t})^2\right)dV, \qquad (3)$$

and the work down by internal viscose fluid is [23]

$$W=\int(F_{fluid})wdA=\int\left(-h\rho_f\left(\frac{\partial^2 w}{\partial t^2}+2\,v_x\frac{\partial^2 w}{\partial x\,\partial t}+{v_x}^2\frac{\partial^2 w}{\partial x^2}\right)\right.$$
$$\left.+\;h\mu\left(\frac{\partial^3 w}{\partial x^2\,\partial t}+\frac{\partial^3 w}{R^2\,\partial\theta^2\,\partial t}+v_x\left(\frac{\partial^3 w}{\partial x^3}+\frac{\partial^3 w}{R^2\,\partial\theta^2\,\partial x}\right)\right)\right)wdA. \qquad (4)$$

Now replacing these in the following expression based on the Hamilton's principal [22, 23]

$$\int_0^t(\delta K-\delta U+\delta W)dt=0, \qquad (5)$$

and defining the following non-dimensional quantities:

Archive of SID

© 2012IAU, Arak Branch

www.SID.ir

$$\{\bar{u},\bar{v},\bar{w}\}=\frac{\{u,v,w\}}{h},\quad \gamma=\frac{h}{l},\quad \xi=\frac{x}{l},\ \beta=\frac{h}{R},\ \bar{C}_{ij}=\frac{C_{ij}}{C_{11}},\ \Phi=\frac{\varphi}{\Phi_0}\ \ \Phi_0=h\sqrt{\frac{C_{11}}{\epsilon_{11}}},$$
$$\bar{e}_{ij}=\frac{e_{ij}}{\sqrt{C_{11}\epsilon_{11}}}\ \bar{\rho}=\frac{\rho_s}{\rho_f},\quad \mu=\frac{\mu_0}{h\sqrt{C_{11}\rho_f}},\ \ V=v_x\sqrt{\frac{\rho_f}{C_{11}}},\ \ \bar{t}=\frac{t}{h\sqrt{\frac{\rho_f}{C_{11}}}}, \tag{6}$$

The four electro-thermo mechanical coupling governing equations of PVDF cylindrical shell conveying viscose fluid, can therefore be written as:

$$\gamma^2\left(\frac{\partial^2\bar{u}}{\partial\xi^2}+\frac{\partial\bar{w}}{\partial\xi}\frac{\partial^2\bar{w}}{\partial\xi^2}\right)+\gamma\beta\bar{C}_{12}\left(\frac{\partial^2\bar{v}}{\partial\xi\partial\theta}+\frac{\partial\bar{w}}{\partial\xi}+\beta\frac{\partial\bar{w}}{\partial\theta}\frac{\partial^2\bar{w}}{\partial\xi\partial\theta}\right)+\beta\bar{C}_{66}\left(\beta\frac{\partial^2\bar{u}}{\partial\theta^2}+\frac{\partial^2\bar{v}}{\partial\xi\partial\theta}+\beta\frac{\partial\bar{w}}{\partial\xi}\frac{\partial^2\bar{w}}{\partial\theta^2}+\frac{\partial\bar{w}}{\partial\xi}+\beta\frac{\partial\bar{w}}{\partial\theta}\frac{\partial^2\bar{w}}{\partial\xi\partial\theta}\right)$$
$$+\gamma^2\bar{e}_{11}\frac{\partial^2\Phi}{\partial\xi^2}=(\bar{\rho})\frac{\partial^2\bar{u}}{\partial\bar{t}^2}, \tag{7}$$

$$\beta\bar{C}_{12}\left(\frac{\partial^2\bar{u}}{\partial\xi\partial\theta}+\frac{\partial\bar{w}}{\partial\xi}\frac{\partial^2\bar{w}}{\partial\xi\partial\theta}\right)+\beta^2\bar{C}_{22}\left(\frac{\partial^2\bar{v}}{\partial\theta^2}+\frac{\partial\bar{w}}{\partial\theta}+\beta\frac{\partial\bar{w}}{\partial\theta}\frac{\partial^2\bar{w}}{\partial\theta^2}\right)+\gamma\bar{C}_{66}\left(\frac{\beta\partial^2\bar{u}}{\partial\xi\partial\theta}+\frac{\partial^2\bar{v}}{\partial\xi^2}+\frac{\beta\partial^2\bar{w}}{\partial\theta\partial\xi}\frac{\partial\bar{w}}{\partial\xi}+\frac{\beta\partial\bar{w}}{\partial\theta}\frac{\partial^2\bar{w}}{\partial\xi^2}\right)$$
$$+\beta\bar{e}_{12}\frac{\partial^2\Phi}{\partial\xi\partial\theta}=\bar{\rho}\frac{\partial^2\bar{v}}{\partial\bar{t}^2}, \tag{8}$$

$$\frac{\gamma^2}{12}\left(-\gamma^2\frac{\partial^4\bar{w}}{\partial\xi^4}-\bar{C}_{12}\beta^2\frac{\partial^4\bar{w}}{\partial\xi^2\partial\theta^2}\right)+\frac{1}{12}\left(-\gamma^2\beta^2\bar{C}_{12}\frac{\partial^4\bar{w}}{\partial\xi^2\partial\theta^2}-\beta^4\bar{C}_{22}\frac{\partial^4\bar{w}}{\partial\theta^4}\right)$$
$$-\frac{\gamma\beta\bar{C}_{12}}{3}\left(\frac{\partial\bar{u}}{\partial\xi}+\frac{\gamma}{2}\left(\frac{\partial\bar{w}}{\partial\xi}\right)^2\right)-\beta\bar{C}_{22}\left(\frac{\partial\bar{v}}{\partial\theta}+\beta\bar{w}+\frac{\beta^2}{2}\left(\frac{\partial\bar{w}}{\partial\theta}\right)^2\right)-\left[\left(\beta^2\alpha_{xx}+\beta^2\bar{C}_{12}\alpha_{\theta\theta}\right)\frac{\partial^2\bar{w}}{\partial\theta^2}\right.$$
$$\left.-\left(\gamma^2\alpha_{xx}+\gamma^2\bar{C}_{12}\alpha_{\theta\theta}\right)\frac{\partial^2\bar{w}}{\partial\xi^2}\right]\Delta T-\left[\frac{\partial^2\bar{w}}{\partial\bar{t}^2}+2\gamma V\frac{\partial^2\bar{w}}{\partial\xi\partial\bar{t}}+\gamma^2V^2\frac{\partial^2\bar{w}}{\partial\xi^2}\right]$$
$$-\mu\left[\gamma^2\frac{\partial^3\bar{w}}{\partial\xi^2\partial\bar{t}}+V\gamma^3\frac{\partial^3\bar{w}}{\partial\xi^3}+\beta^2\left(\frac{\partial^3\bar{w}}{\partial\theta^2\partial\bar{t}}+V\gamma\frac{\partial^3\bar{w}}{\partial\theta^2\partial\xi}\right)\right]+\gamma\beta\bar{e}_{12}\frac{\partial\Phi}{\partial\xi}=\bar{\rho}\frac{\partial^2\bar{w}}{\partial\bar{t}^2}, \tag{9}$$

$$-\frac{\partial^2\Phi}{\partial\xi^2}+\bar{e}_{11}\left(\frac{\partial^2\bar{u}}{\partial\xi^2}+\gamma\frac{\partial\bar{w}}{\partial\xi}\frac{\partial^2\bar{w}}{\partial\xi^2}\right)+\frac{\beta\bar{e}_{12}}{\gamma}\left(\frac{\partial^2\bar{v}}{\partial\xi\partial\theta}+\frac{\partial\bar{w}}{\partial\xi}+\frac{\beta}{\gamma}\frac{\partial\bar{w}}{\partial\theta}\frac{\partial^2\bar{w}}{\partial\xi\partial\theta}\right)=0. \tag{10}$$

2.2 HDQM

These four governing equations Eqs. (7)–(10) are discetized using HDQM, so that they are solved considering the associated boundary conditions to obtain vibration and instability of the viscose-fluid-conveying cylindrical shell made from PVDF. The HDQM approximates the partial derivative of a function F (representing $\bar{u}$, $\bar{v}$, $\bar{w}$ and Φ), with respect to two spatial variables (ξ and θ) at a given discrete point (ξ_i,θ_i) , as a weighted linear sum of the function values at all discrete points chosen in the solution domain ($0<\xi<L$, $0<\theta<2\pi$) with $N_\xi\times N_\theta$ grid points along ξ and θ axes, respectively. Then, the nth-order partial derivative of $F(\xi,\theta)$ with respect to ξ , the mth-order partial derivative of $F(\xi,\theta)$ with respect to θ and the (n + m)th-order partial derivative of $F(\xi,\theta)$ with respect to both ξ and θ is expressed discretely at the point (ξ_i,θ_i) as [24]

© 2012 IAU, Arak Branch

www.SID.ir

Archive of SID

$$\frac{d^n F(\xi_i,\theta_j)}{d\xi^n} = \sum_{k=1}^{N_\xi} A_{ik}^{(n)} F(\xi_k,\theta_j) \qquad n=1,...,N_\xi -1, \tag{11}$$

$$\frac{d^m F(\xi_i,\theta_j)}{d\theta^m} = \sum_{l=1}^{N_\theta} B_{jl}^{(m)} F(\xi_i,\theta_l) \qquad m=1,...,N_\theta -1, \tag{12}$$

$$\frac{d^{n+m} F(\xi_i,\theta_j)}{d\xi^n d\theta^m} = \sum_{k=1}^{N_\xi}\sum_{l=1}^{N_\theta} A_{ik}^{(n)} B_{jl}^{(m)} F(\xi_k,\theta_l), \tag{13}$$

where $A_{ik}^{(n)}$ and $B_{jl}^{(m)}$ are the weighting coefficients associated with n[th]-order partial derivative of $F(\xi,\theta)$ with respect to ξ at the discrete point ξ_i and m[th]-order derivative with respect to θ at θ_i, respectively, whose recursive formula are described in [21]. Chebyshev polynomials [25] was used to determine the positions of the grid points. As for the displacement components, the following solutions may be assumed [26] in the free vibration analysis

$$\overline{u}(x,y,t) = \overline{u}(x,y)e^{\lambda\overline{t}}, \tag{14}$$

$$\overline{v}(x,y,t) = \overline{v}(x,y)e^{\lambda\overline{t}}, \tag{15}$$

$$\overline{w}(x,y,t) = \overline{w}(x,y)e^{\lambda\overline{t}}, \tag{16}$$

where λ is the(Fundamental) natural frequency. Applying HDQM and using Eqs. (14)-(16) to Eqs. (7)–(10) results the following governing equations

$$\begin{aligned}&(\gamma^2)\Big((I_\theta \otimes A^{(2)})\overline{u} + \big[(I_\theta \otimes A^{(1)})\overline{w} \circ (I_\theta \otimes A^{(2)})\overline{w}\big]\Big)\\&+\gamma\beta\overline{C}_{12}\Big((B^{(1)} \otimes A^{(1)})\overline{v} + (I_\theta \otimes A^{(1)})\overline{w} + \beta\big[(B^{(1)} \otimes I_\xi)\overline{w} \circ (B^{(1)} \otimes A^{(1)})\overline{w}\big]\Big)\\&+\beta\overline{C}_{66}\Big(\beta(B^{(1)} \otimes I_\xi)\overline{u} + \big(B^{(1)} \otimes A^{(2)}\big)\overline{v} + \beta\Big[(I_\theta \otimes A^{(1)})\overline{w} \circ \big((B^{(2)} \otimes I_\xi)\overline{u}\Big]\\&+(I_\theta \otimes A^{(1)})\overline{w} + \beta\big[(B^{(1)} \otimes I_\xi)\overline{w} \circ (B^{(1)} \otimes A^{(2)})\overline{v}\big] + \gamma^2\overline{e}_{11}(I_\theta \otimes A^{(1)})\Phi = \overline{\rho}\,\Omega^2\,\overline{u},\end{aligned} \tag{17}$$

$$\begin{aligned}&\beta\overline{C}_{12}\Big((B^{(1)} \otimes A^{(1)})\overline{u} + \big[(I_\theta \otimes A^{(1)})\overline{w} \circ (B^{(1)} \otimes A^{(1)})\overline{w}\big]\Big)\\&+\beta^2\overline{C}_{22}\Big((B^{(2)} \otimes I_\xi)\overline{v} + (B^{(1)} \otimes I_\xi)\overline{w} + \beta\big[(B^{(1)} \otimes I_\xi)\overline{w} \circ (B^{(2)} \otimes I_\xi)\overline{w}\big]\Big)\\&+\gamma\overline{C}_{66}\Big(\beta(B^{(1)} \otimes A^{(1)})\overline{u} + (I_\theta \otimes A^{(2)})\overline{v} + \beta\big[(I_\theta \otimes A^{(1)})\overline{w} \circ (B^{(1)} \otimes A^{(1)})\overline{w}\big]\\&+\beta\big[(B^{(1)} \otimes I_\xi)\overline{w} \circ (I_\theta \otimes A^{(2)})\overline{w}\big] + \beta\overline{e}_{12}(B^{(1)} \otimes A^{(1)})\Phi = \overline{\rho}\;\Omega^2\;\overline{v},\end{aligned} \tag{18}$$

$$\begin{aligned}&\frac{\gamma^2}{12}\Big(\gamma^2(I_\theta \otimes A^{(4)})\overline{w} - \overline{C}_{12}\beta^2(B^{(2)} \otimes A^{(2)})\overline{w}\Big) + \frac{1}{12}\Big(\gamma^2\beta^2\overline{C}_{12}(B^{(2)} \otimes A^{(2)})\overline{w} - \beta^4\overline{C}_{22}(B^{(4)} \otimes I_\xi)\overline{w}\Big)\\&-\frac{\gamma\beta\overline{C}_{12}}{3}\left((I_\theta \otimes A^{(4)})\overline{u} + \frac{\gamma}{2}\big[(I_\theta \otimes A^{(1)})\overline{w} \circ (I_\theta \otimes A^{(1)})\overline{w}\big]\right) - \beta\,\overline{C}_{22}\Big((B^{(1)} \otimes I_\xi)\overline{v} + \beta\;\overline{w}\\&+\frac{\beta^2}{2}\big[(B^{(1)} \otimes I_\xi)\overline{w} \circ (B^{(1)} \otimes I_\xi)\overline{w}\big]\Big) + \Big(\big(\beta^2\,\alpha_{xx} + \beta^2\,\overline{C}_{12}\,\alpha_{\theta\theta}\big)(B^{(1)} \otimes I_\xi)\overline{w} + \big(\gamma^2\,\alpha_{xx} + \gamma^2\overline{C}_{12}\,\alpha_{\theta\theta}\big)\\&(I_\theta \otimes A^{(2)})\overline{w}\Big)\Delta T - \Big(\Omega^2\,\overline{w} + 2\gamma\;V(I_\theta \otimes A^{(1)})\overline{w} + \gamma^2 V^2(I_\theta \otimes A^{(2)})\overline{w}\Big) - \overline{\mu}\,\Big(\gamma^2(I_\theta \otimes A^{(2)})\Omega\overline{w}\\&+V\gamma^3(I_\theta \otimes A^{(3)})\overline{w} + \beta^2\Big((B^{(2)} \otimes I_\xi)\Omega\overline{w} + V\gamma(B^{(1)} \otimes A^{(1)})\overline{w}\Big)\Big) + \gamma\;\beta\;\overline{e}_{12}(I_\theta \otimes A^{(1)})\Phi = \overline{\rho}\Omega^2\overline{w},\end{aligned} \tag{19}$$

© 2012IAU, Arak Branch

www.SID.ir

Archive of SID

$$-(I_\theta \otimes A^{(2)})\Phi + \bar{e}_{11}\left((I_\theta \otimes A^{(2)})\bar{u} + \gamma\left[(I_\theta \otimes A^{(1)})\bar{w} \circ (I_\theta \otimes A^{(2)})\bar{w}\right]\right)$$
$$+\frac{\beta \bar{e}_{12}}{\gamma}\left((B^{(1)} \otimes A^{(1)})\bar{v} + (I_\theta \otimes A^{(1)})\bar{w} + \frac{\beta}{\gamma}\left[(B^{(1)} \otimes I_\xi)\bar{w} \circ (B^{(1)} \otimes A^{(1)})\bar{w}\right]\right) = 0, \quad (20)$$

where $\Omega = (\lambda/h)\sqrt{C_{11}/\rho_f}$ is the dimensionless natural frequency, symbols $\otimes$ and $\circ$ indicate Kronecker and Hadamard products, respectively [27], I_ξ and I_θ are the unit matrices. The associated mechanical clamped and free electrical boundary conditions at both ends of the shell, in HDQM form, may be written in dimensionless form as:

$$\begin{cases} \bar{w}_{i1} = \bar{v}_{i1} = \bar{u}_{i1} = \Phi_{i1} = 0, & \sum_{j=1}^{N_\theta} A_{2j} w_{ji} = 0 \\ \bar{w}_{N_x i} = \bar{v}_{N_x i} = \bar{u}_{N_x i} = \Phi_{N_x i} = 0, & \sum_{j=1}^{N_\theta} A_{(N_x-1)j} w_{ji} = 0 \end{cases} \quad for \quad i = 1 \ldots N_\theta. \quad (21)$$

Applying these boundary conditions into the above four governing equations, Eqs. (17-20), the following constitutive matrix equation is obtained

$$\left(\left[\underbrace{K_L + K_{NL}}_{K}\right] + \Omega[C] + \Omega^2[M]\right)\begin{Bmatrix}\{d_b\} \\ \{d_d\}\end{Bmatrix} = 0, \quad (22)$$

where the subscript b denotes the elements associated with the boundary points while subscript d is the remainder elements. Eq. (22), however, is a generalized eigenvalue equation, and to reduce it to the standard form, assume $Z = \{\dot{\bar{u}}_d, \bar{u}_d, \dot{\bar{v}}_d, \bar{v}_d, \dot{\bar{w}}_d, \bar{w}_d\}^T$, then

$$[A]\{Z\} = \Omega\{Z\}, \quad (23)$$

where

$$[A] = \begin{bmatrix} [0] & [I] \\ -\left[M_{eq}^{-1}K_{eq}\right] & -\left[M_{eq}^{-1}C_{eq}\right] \end{bmatrix}, \quad (24)$$

where $[I]$and $[0]$ are the unit and zeroes matrixes. However, the frequencies obtained from the solution of Eq. (24) are complex due to the damping caused by the presence of the viscous fluid. Hence, the results would comprise of two parts, the real part corresponding to the system damping, and the imaginary part representing the system natural frequencies. These are discussed in the next section.

3 RESULTS AND DISCUSSION

A code was written for the HDQM mathematical model expressed above ,using MATLAB software, where the effect of parameters such as fluid velocity and geometry and material type of the shell, on the nonlinear resonance frequencies and instability of the PVDF cylindrical shell reinforced with BNNTs and conveying viscose fluid, are investigated. The material properties PVDF as a matrix were found to be as follows [13]:

$$C_{11} = 238.24(Gpa), C_{22} = 23.6(GPa), C_{12} = 3.98(GPa), C_{66} = 6.43(GPa), e_{11} = -0.135(C/m^2), e_{12} = -0.145(C/m$$
$$\alpha_x = 7.1e-5(1/K), \alpha_\theta = 7.1e-5(1/K)$$

and employing DWBNNTs as the matrix reinforcer provides the following material properties [13]

Archive of SID
www.SID.ir

$$E = 1.8(Tpa), \upsilon = 0.34, e_{11} = 0.95(C/m^2), \alpha_x = 1.2e-6(1/K), \alpha_\theta = 0.6e-6(1/K).$$

In the absence of similar publications in the literature covering the same scope of the problem, one can not directly validate the results found here. However, the present work could be partially validated based on a simplified analysis suggested by Amabili [22] and Zhou [28].

Second, vibration and instability of simply supported classical cylindrical shells conveying water are investigated where the nonlocal parameter, electric field , and vdW force are ignored. The structure parameters of the classical shell assumed are $h/R = 0.01$, $L/R = 2$, $E = 206\,GPa$, $\nu = 0.3$, $\rho = 7850\ Kg/m^3$ and the water density $\rho_f = 1000\ Kg/m^3$. A non-dimensional fluid velocity is defined as $u_f = V/\{\pi^2/L[D/\rho h]\}^{0.5}$, with $D = Eh^3/[12(1-\nu^2)]$, and a non-dimensional eigenvalue is also defined as $\omega = \lambda/\{\pi^2/L^2[D/\rho h]\}^{0.5}$, where λ is the eigenvalue. Figs. 2a and 2b illustrate the imaginary and real parts of frequency versus dimensionless flow velocity, respectively. As can be seen, the obtained results are the same as those expressed in [22, 28], indicating validation of our work. In this study the internal fluid is modeled by Nervier-stocks relation and the effect of viscosity is considered which makes a little difference between the results of Zhou [28], Amabili [22] and the present work .

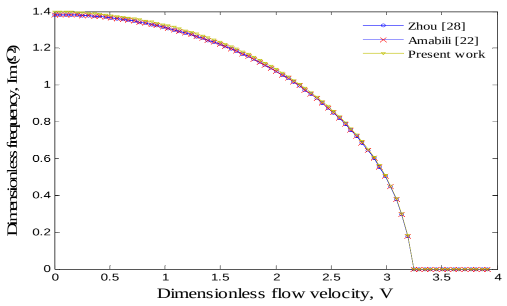

Fig. 2a
The imaginary part of frequency versus dimensionless flow velocity for simply supported classical cylindrical shells conveying water.

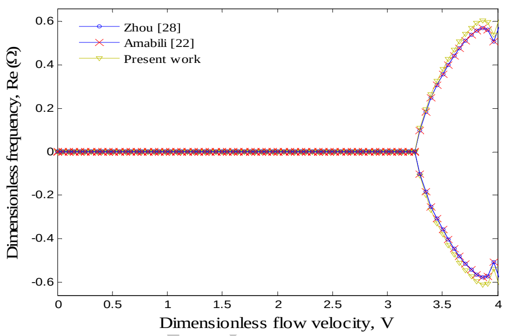

Fig. 2b
The real part of frequency versus dimensionless flow velocity for simply supported classical cylindrical shells conveying water.

Figs. 3 and 4 demonstrate in dimensionless forms, the natural frequency ($\mathrm{Im}(\omega)$) and damping ratio ($\mathrm{Re}(\omega)$) versus fluid velocity (*V*) for the first four vibration modes of the system. As can be seen, in general, $\mathrm{Im}(\omega)$ is directly related to the vibration modes. $\mathrm{Im}(\omega)$ also reduces with increased *V*, and in the first mode this approaches zero at the critical velocity of *V*=2.92, where divergence instability occurs due to pitchfork bifurcation of $\mathrm{Re}(\omega)$. (It is interesting to note that at this speed, the 2nd, 3rd and 4th modes still remain stable.) At 2.92<*V*<5.54, shell absorbs energy from the fluid and converts it to higher frequency vibration. For *V* >5.54, the system tends to regain its stability.

Increasing *V* beyond 5.54 for the 2nd mode, tends $\mathrm{Im}(\omega)$ from zero to positive values, so that at *V*=5.56, 1st and 2nd modes combine while $\mathrm{Re}(\omega)$ remains non-zero. At this state, the shell becomes unstable with a flutter instability. Figs. 5 and 6 illustrate in dimensionless forms, changes in $\mathrm{Re}(\omega)$ and $\mathrm{Im}(\omega)$ versus the *V*, for different β 's (defined as ratio of thickness to radius of the shell) and material types. Clearly, increase in β leads to

www.SID.ir

increased natural frequency and enhanced stability. Higher values of β corresponds to the increased stiffness of the shell on the one hand, while from another point of view it leads to increased smartness (or electric potential), making the system more suitable for sensors and actuator applications. Comparing different material types investigated here (i.e. smart PVDF and non-smart polyethylene (PE)), it is clear that PVDF improves significantly the stability and vibration of the system. This suggests that in gas transmission lines, where safety and stability of the lines are of paramount importance, application of PVDF pipes is preferred to those of the conventional PE.

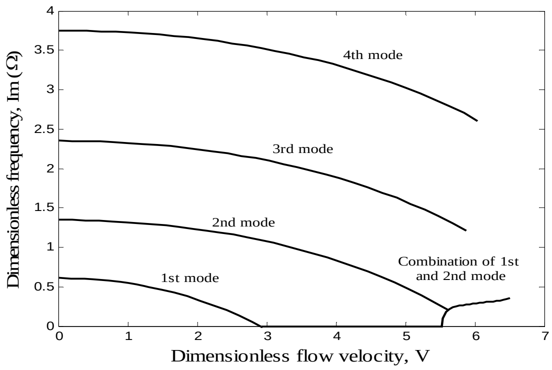

Fig. 3
The imaginary component of the dimensionless frequency, as a function of fluid velocity, for the lowest four modes of a clamped-clamped smart composite cylindrical shell conveying viscose fluid.

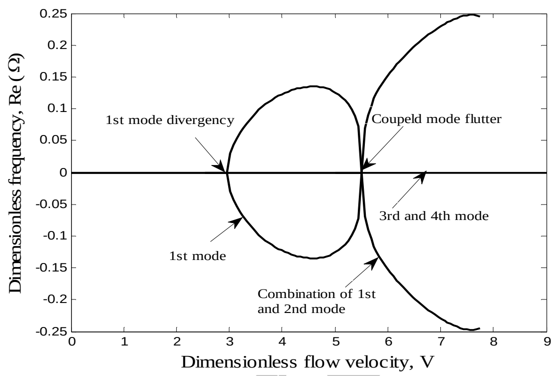

Fig. 4
The real component of the dimensionless frequency, as a function of fluid velocity, for the lowest four modes of a clamped-clamped smart composite cylindrical shell conveying viscose fluid.

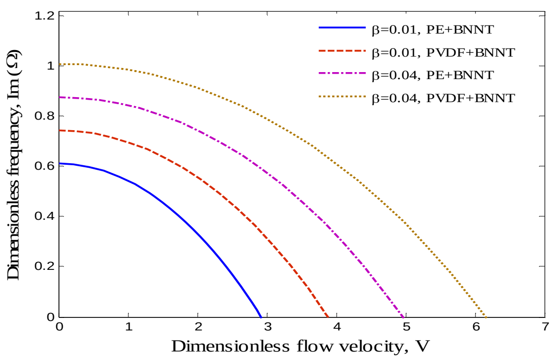

Fig. 5
Effect of β and material types of the smart composite cylindrical shell on the imaginary component of the dimensionless frequency for the first mode.

© 2012 IAU, Arak Branch

www.SID.ir

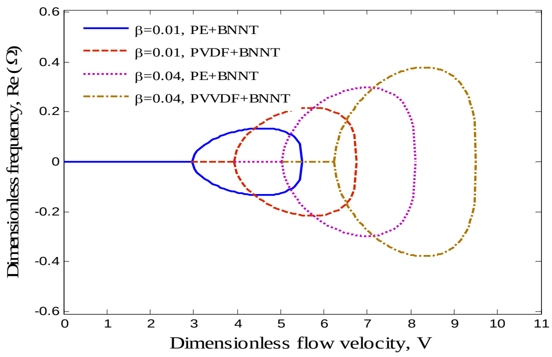

Fig. 6
Effect of β and material types of the smart composite cylindrical shell on the real component of the dimensionless frequency for the first mode.

4 CONCLUSIONS

This paper investigates the electro-thermo-mechanical nonlinear vibration and instability of a cylindrical shell made with PVDF and reinforced by BNNTs, carrying a viscose fluid. The HDQ method is employed to discretize the governing equations, which are then solved to obtain the resonant frequencies and critical fluid velocity with clamped boundary conditions. The influences of fluid velocity, geometrical parameter and material types of shell on the nonlinear vibration and flow-induced instability of the shell are discussed. The results indicate that in the 1st mode, divergence instability occurs in the system at the speed V=2.92, while 2nd, 3rd and 4th modes still remain stable, reaching flutter instability at V=5.56. Also, increase in β (the ratio of thickness to radius of the shell) leads to increased in natural frequency and enhanced stability of the system. Application of a smart material such as PVDF improves significantly the stability and vibration of the system.

ACKNOWLEDGEMENTS

The authors would like to thank the referees for their valuable comments. They would also like to thank the Thermoelasticity Center of Excelence for their financial support. The authors are grateful to University of Kashan for supporting this work by Grant No. 65475/49.

REFERENCES

[1] Païdoussis M.P., Denise J.P., 1972, Flutter of thin cylindrical shells conveying fluid, *Journal of Sound and* Vibration **20**: 9-26.
[2] Amabili M., Garziera R., 2002, Vibrations of circular cylindrical shells with nonuniform constraints, elastic bed and added mass; Part II: shells containing or immersed in axial flow, *Journal of Fluids and Structures* **16**: 31–51.
[3] Païdoussis M.P., 2004, *Fluid–Structure Interactions: Slender Structures and Axial Flow*, Elsevier Academic Press, London.
[4] Kotsilkova R., 2007, *Thermoset Nanocomposites for Engineering Applications*, Smithers, USA.
[5] Merharihybrid L., 2002, *Nanocomposites for Nanotechnology*, Springer Science, New York.
[6] Yu V., Christopher T., Bowen R., 2009, *Electromechanical Properties in Composites Based on Ferroelectrics*, Springer-Verlag, London.
[7] Ghorbanpour Arani A., Kolahchi R., Mosallaie Barzoki A.A., Loghman, A., 2011, Electro-thermomechanical behaviors of FGPM spheres using analytical method and ANSYS software, *Applied Mathematical Modelling* **36**: 139–157.
[8] Ghorbanpour Arani A., Kolahchi R., Mosallaie Barzoki A.A., 2011, Effect of material inhomogeneity on electro-thermo-mechanical behaviors of functionally graded piezoelectric rotating cylinder, *Applied Mathematical Modelling* **35**: 2771–2789.
[9] Bent A.A., Hagood N.W., Rodgers J.P., 1995, Anisotropic actuation with piezoelectric fiber composites, *Journal of Material Sysistem and Structures* **6**: 338–349.

© 2012IAU, Arak Branch

Archive of SID
www.SID.ir

[10] Matsuna H., 2007, Vibration and buckling of cross-ply laminated composite circular cylindrical shells according to a global higher-order theory, *International Journal of Mechanical Science* **49**: 1060-1075.

[11] Kadoli R., Ganesan N., 2003, Free vibration and buckling analysis of composite cylindrical shells conveying hot fluid, *Composite Structures* **60**: 19–32.

[12] Messina A., Soldatos K.P., 1999, Vibration of completely free composite plates and cylindrical shell panels by a higher-order theory, *International Journal of Mechanical Science* **41**: 891-918.

[13] Mosallaie Barzoki A.A., Ghorbanpour Arani A., Kolahchi R., Mozdianfard M.R., 2011, Electro-thermo-mechanical torsional buckling of a piezoelectric polymeric cylindrical shell reinforced by DWBNNTs with an elastic core, *Applied Mathematical Modeling* **36**: 2983–2995.

[14] Bellman R.E., Casti J., 1971, Differential quadrature and long-term integration, *Journal of Mathematics Analysis and Application* **34**: 235-238.

[15] Bellman R.E., Kashef B.G., Casti J., 1972, Differential quadrature: A technique for the rapid solution of nonlinear partial differential equations, *Journal of Computational and Physics* **10**: 40-52.

[16] Farsa J., Kukreti A.R., Bert C.W., 1993, Fundamental frequency analysis of laminated rectangular plates by differential quadrature method, *International Journal of Numerical Methods and Engineering* **36**: 2341–56.

[17] Jang S.K., Bert C.W., Striz A.G., 1989, Application of differential quadrature to static analysis of structural components, *International Journal of Numerical Methods Engineering* **28**: 561–77.

[18] Sherbourne A.N., Pandey M.D., 1991, Differential quadrature method in the buckling analysis of beams and composite plates, *Computers and Structures* **40**: 903–913.

[19] Striz A.G., Wang X., Bert C.W., 1995, Harmonic differential quadrature method and applications to analysis of structural components, *Acta Mechanica* **111**: 85–94.

[20] Liew K.M., Teo T.M., Han J.B., 1999, Comparative accuracy of DQ and HDQ methods for three-dimensional vibration analysis of rectangular plates, *International Journal of Numerical Methods and Engineering* **45**: 1831–1848.

[21] Civalek Ö., 2004, Application of differential quadrature (DQ) and harmonic differential quadrature (HDQ) for buckling analysis of thin isotropic plates and elastic columns, *Engineering Structures* **26**: 171–186.

[22] Amabili M., 2008, *Nonlinear Vibrations and Stability of Shells and Plates*, Cambridge University Press, USA.

[23] Wang L., Ni Q., 2009, A reappraisal of the computational modelling of carbon nanotubes conveying viscous fluid, *Mechanics Research Communications* **36**: 833–837.

[24] Liew K.M., Han J.B., Xiao Z.M., 1996, Differential Quadrature Method for Thick Symmetric Cross-Ply Laminates with First-Order Shear Flexibility, *International Journal of Solids and Structures* **33**: 2647-2658.

[25] Shu C., Richards B.E., 1992, Application of generalized differential quadrature to solve two-dimensional incompressible Navier– Stokes equations, *International Journal of Numerical Methods in Fluids* **15**: 791–798.

[26] Malekzadeh P., 2008, Nonlinear free vibration of tapered Mindlin plates with edges elastically restrained against rotation using DQM, *Thin-Walled Structures* **46**: 11–26.

[27] Chen W., Shu C., He W., Zhong, T., 2000, The applications of special matrix products to differential quadrature solution of geometrically nonlinear bending of orthotropic rectangular plates, *Computers and Structures* **74**: 65–76.

[28] Zhou X., 2012, Vibration and stability of ring-stiffened thin-walled cylindrical shells conveying fluid, *Acta Mechanica Solida Sinica* **25**:168–176.

Archive of SID

© 2012 IAU, Arak Branch

www.SID.ir